IOP Publishing Superconductor Science and Technology
Supercond. Sci. Technol. **31** (2018) 015016 (8pp) https://doi.org/10.1088/1361-6668/aa98d7

Quasi-two-dimensional vortex–glass transition and the critical current density in TiO epitaxial thin films

Chao Zhang[1], Feixiang Hao[1], Xiang Liu[1], Yunjie Fan[1], Tianyi Wang[1], Yuewei Yin[1,5] and Xiaoguang Li[1,2,3,4,5]

[1] Hefei National Laboratory for Physical Sciences at the Microscale, Department of Physics, University of Science and Technology of China, Hefei 230026, People's Republic of China
[2] Key Laboratory of Materials Physics, Institute of Solid State Physics, CAS, Hefei 230026, People's Republic of China
[3] School of Physics and Materials Science, Anhui University, Hefei, Anhui 230601, People's Republic of China
[4] Collaborative Innovation Center of Advanced Microstructures, Nanjing 210093, People's Republic of China

E-mail: lixg@ustc.edu.cn and yyw@ustc.edu.cn

Received 8 September 2017, revised 4 November 2017
Accepted for publication 7 November 2017
Published 6 December 2017

Abstract

There are many fascinating properties in titanium oxides such as the enhanced superconductivity in cubic TiO epitaxial thin films with the superconducting transition temperature T_c^{onset} of 7.65 K, which is much higher than that of the bulk polycrystalline TiO. To explore the superconductivity of the TiO thin films in more detail, we investigated the magnetic field and temperature dependences of the current–voltage (I–V) characteristics and the critical current density J_c in magnetic fields perpendicular to the film surface. The I–V curves show a quasi-two-dimensional vortex glass (VG) scaling collapse in different magnetic fields, and a vortex phase diagram is constructed from the VG and vortex liquid regions to the normal state. Through the critical current density investigation, we found that δl pinning dominates the pinning behavior, which is in accordance with the analyzed results of the vortex pinning force associated with defects in the film, such as grain boundaries. The findings of the magnetic phase diagram and critical current properties should be helpful for practical applications of the TiO family.

Supplementary material for this article is available online

Keywords: TiO superconducting thin films, vortex–glass transition, critical current density, vortex pinning behavior

(Some figures may appear in colour only in the online journal)

1. Introduction

The magnetic phase diagram and critical current properties of various superconductors have been actively investigated due to their importance in both physics and applications [1–3]. The most intriguing phenomena in superconductors includes the different possible vortex states in the H–T phase diagram, and the nature of the thermodynamic transitions among the different phases, especially the phase transition from the vortex glass (VG) to vortex liquid phase in magnetic fields [4–6]. The VG phase [7] has been the central issue for understanding the physics of the mixed state of type-II superconductors [8], and can be studied through measuring the current–voltage (I–V) characteristics at different temperatures in magnetic fields [9].

[5] Authors to whom any correspondence should be addressed.

However, owing to the complicated nature of superconductivity, the *I–V* characteristics also show complex features. For example, the *I–V* characteristics demonstrated a good agreement with the three-dimensional (3D) VG theory for both polycrystalline bulk [10] and thin film [11] samples of MgB_2, whereas other studies proved that the *I–V* curves scaled well according to the quasi-two-dimensional (quasi-2D) VG theory instead of the 3D model [12]. Meanwhile, for high-quality epitaxial $YBa_2Cu_3O_{7-\delta}$ films, a crossover from 3D to a pure 2D VG transition was found by changing the oxygen content in the films [13]. It should be noted that a quasi-2D VG phase transition can be observed in the *I–V* isotherms for many kinds of superconductors, such as Bi- and Tl-based cuprate superconductors [14–18], as well as Nb/Cu superlattices [19].

On the other hand, the critical current density (J_c) associated with the vortex pinning behavior is a parameter of primary importance for potential applications [20, 21]. The critical current density J_c and pinning mechanism can be revealed via measuring the *I–V* characteristics in magnetic fields. As for the decay of critical current density with temperature, two basic pinning mechanisms were proposed [22, 23]. One is the δTc pinning provided by spatial variations of the Ginzburg–Landau parameter in the superconducting matrix; the other is δl pinning due to the spatial fluctuation of the charge carrier mean free path induced by the non-superconducting defects embedded in the superconducting matrix [22, 24]. The different pinning natures are correlated with the microstructures and defects in the sample.

Recently, we prepared titanium monoxide (TiO) epitaxial thin films exhibiting an enhanced superconducting transition temperature with zero-resistance $T_{c0} \sim 5.50$ K, higher than the bulk TiO $T_{c0} \sim 2.8$ K reported by Huang's group [25], and found that the superconducting properties of TiO are very sensitive to sample synthesis conditions. The superconducting properties of the TiO epitaxial thin films were also systematically investigated under hydrostatic pressures up to 2.13 GPa, and it was found that T_{c0} decreases with increasing pressure [26]. However, the mechanism of enhanced superconductivity, pinning behavior, and vortex phase diagram of TiO epitaxial thin films still remain unclear. Therefore, it is necessary to investigate the vortex dynamics in high-quality TiO epitaxial thin films and to reveal the intrinsic properties of the vortex matter in this interesting superconducting system. Through investigations of the *I–V* characteristics and critical current density J_c of TiO thin films in different magnetic fields, we found a typical quasi-2D vortex–glass transition behavior, and constructed the vortex phase diagram for the TiO system. The temperature dependences of critical current densities $J_c(T)$ in different magnetic fields were analyzed by assuming the coexistence of δT_c and δl pinning mechanisms.

2. Experimental details

TiO thin films with a thickness of ~80 nm were epitaxially grown on (0001)-oriented α-Al_2O_3 single crystalline substrates by a pulsed laser deposition technique. The synthesis method and structure characterization of the high-quality TiO thin films are described in detail elsewhere [27]. For the transport measurements, a Hall bar of $800\,\mu m \times 160\,\mu m \times 80$ nm ($a \times b \times c$) was fabricated by ultraviolet lithography and Ar ion milling. Electrical transport measurements were performed for the magnetic fields perpendicular to the surface of the TiO films in a Physical Property Measurement System (PPMS-9, Quantum Design). The *I–V* curves were measured by a Keithley 6221 current source and a Keithley 2182A nanovoltmeter. The sample temperature stability was kept within 0.05 K during the *I–V* measurements.

3. Results and discussion

Figure 1 shows the current–voltage (*I–V)* isotherms measured at 0.5, 3.0, 5.0, and 7.0 T for the TiO epitaxial thin films. According to the VG phase theory, a straight *I–V* curve found on the *log–log* scale plot indicates the vortex liquid–glass transition temperature (T_g) (the black solid line shown in all panels of figures 1(a)–(d)). The *I–V* isotherms show positive curvatures above T_g, and negative curvatures below T_g [28]. The nonlinear *I–V* curves near the VG transition temperature T_g for a dimensional system have a general scaling form as follows [29]:

$$V(I) = I\xi_g{}^{D-2-z}\chi_\pm(I\xi_g{}^{D-1}/T). \tag{1}$$

Here, the correlation length ξ_g is expected to behave as $|(T - T_g)/T_g|^{-\nu}$, and ν and z are static and dynamical critical exponents, respectively. $\chi_\pm$ are the scaling functions for the temperatures above and below T_g (often taken simply linear as $\chi_\pm(x) \sim x$). D denotes the dimensionality of the system, with a value of 3 for 3D and 2 for quasi-2D [14]. By applying $D = 2$ or 3, equation (1) allows the collapse of the *I–V* isothermals and the visualization of the scaling function $\chi_\pm$ by plotting the function $Y = (V/I)\,|1 - T/T_g|^{-\nu(z+2-D)}$ *versus* $X = I/(T\,|1 - T/T_g|^{\nu(D-1)})$. Here, the value of the critical exponent z is obtained from the straight *I–V* isotherm curve by fitting the data at T_g with $V(I; T = T_g) \sim I^{(z+1)/(D-1)}$ [29]. The exponent ν is calculated by fitting the linear resistivity at a small current for each isotherm above T_g, and the low current linear resistivity ρ_{lin} obeys the following power law [29]:

$$\rho_{lin} \sim (T - T_g)^{\nu(z+2-D)}. \tag{2}$$

Here, ρ_{lin} equals zero in the VG regime below T_g, where the isotherms exhibit downward curvatures in the double-logarithmic plot of *I–V* curves.

For our sample, a set of nice collapses of the *I–V* isothermals can be achieved with $D = 2$; two representative collapses in magnetic fields of 0.5 T and 4.0 T are shown in figure 2. Table 1 shows the T_g, z, and ν values in different magnetic fields for $D = 2$. The magnitudes of the exponents z

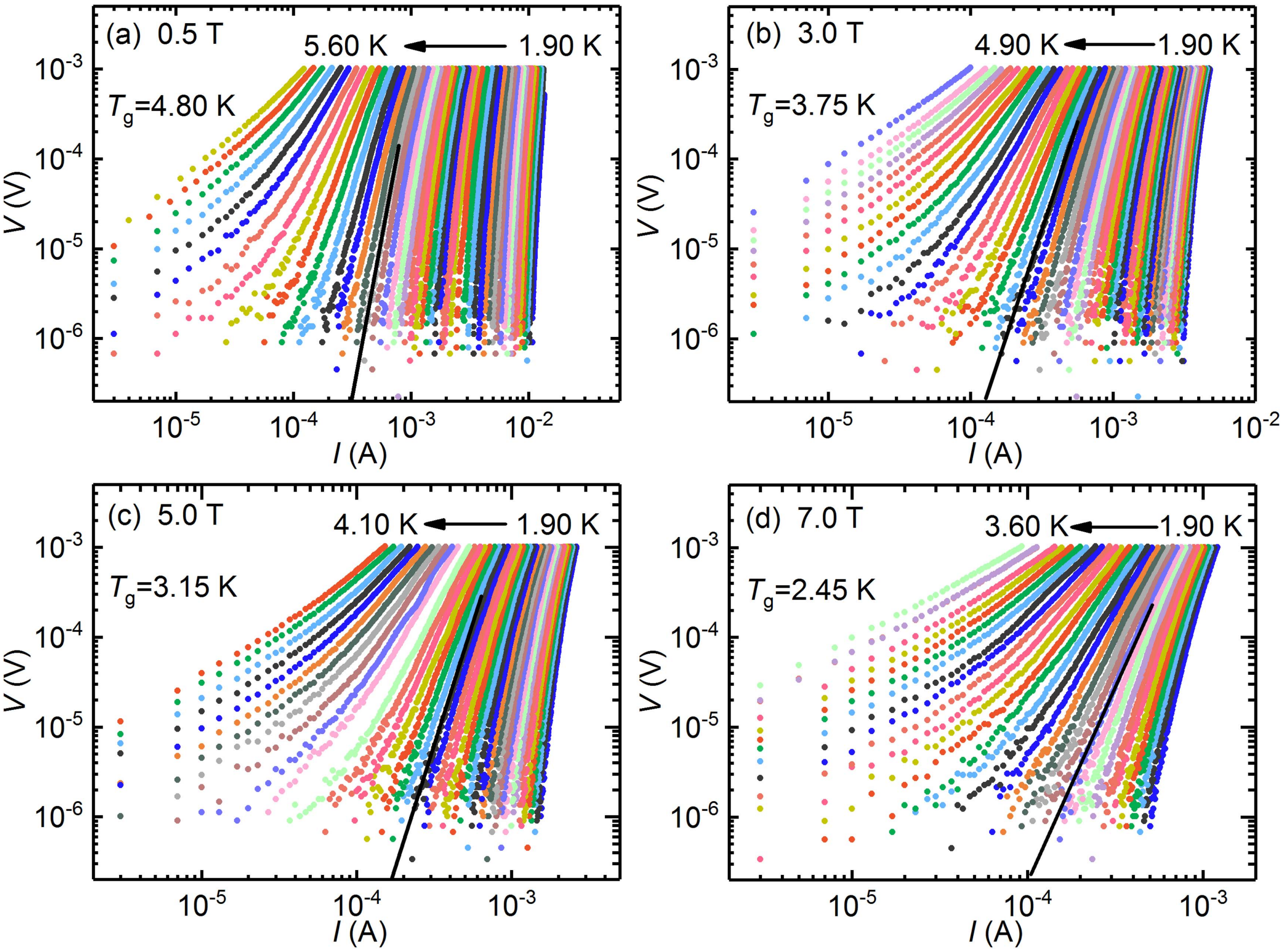

Figure 1. (a)–(d) *I*–*V* curves for the TiO epitaxial thin films at different temperatures with a temperature interval ΔT of 0.05 K under the magnetic fields of 0.5, 3.0, 5.0, and 7.0 T, respectively. The black solid lines represent the vortex liquid–glass transition temperature T_g.

and v decrease with increasing magnetic fields. Meanwhile, for the scaling with $D = 3$, the z values are much higher than the reasonable range, and the *I*–*V* curves show worse collapses. Our scaling results show that the quasi-2D VG scaling theory is well applied for the TiO epitaxial thin films, which is similar to those obtained in ~100 nm MgB_2 films [12], indicating that the 80 nm TiO epitaxial thin film may have two-dimensional superconductivity.

Based on the results of scaling analysis of the *I*–*V* characteristics mentioned above, and the *R*–*T* broadening curves in different magnetic fields shown in figure 3(a), we constructed the magnetic phase diagram, which is important for the application of TiO thin films. Figure 3(b) shows the upper critical fields $H_{c2}(T)$ defined by the resistivity drop to 90% of the normal state resistance. The irreversibility field H_{irr}, a characteristic magnetic field at which the magnetic and flux–flow behaviors of a superconductor change from irreversible to reversible [30], is also obtained by the resistivity drop to 0.01% of the normal state resistance [22]. Considering the contributions of the orbital pair-breaking effect and the spin-paramagnetic pair-breaking effect in magnetic fields, the temperature dependences of $H_{c2}(T)$ can be calculated by using the Werthamer–Helfand–Hohenberg (WHH) theory [31]:

$$\ln\frac{1}{t} = \left(\frac{1}{2} + \frac{i\lambda_{so}}{4\gamma}\right)\psi\left(\frac{1}{2} + \frac{\bar{h} + \lambda_{so}/2 + i\gamma}{2t}\right) + \left(\frac{1}{2} - \frac{i\lambda_{so}}{4\gamma}\right)\psi\left(\frac{1}{2} + \frac{\bar{h} + \lambda_{so}/2 - i\gamma}{2t}\right) - \psi\left(\frac{1}{2}\right). \quad (3)$$

Here, $t = T/T_c$, $\bar{h} = \frac{4H_{c2}}{\pi^2(-dH_{c2}/dt)_{t=1}}$, $\gamma = [(\alpha\bar{h})^2 - (\lambda_{so}/2)^2]^{1/2}$, α is the Maki parameter representing the relative strength of spin and orbital pair breakings, and λ_{so} is the spin–orbit scattering constant. Equation (3) fits the experimental data very well with the fitting parameters $\alpha = 3.4$, $\lambda_{so} = 2.0$, and $H_{c2}(0) = 13.50$ T, as shown in figure 3(b). We can see that both the orbital and Pauli-paramagnetic pair-breaking effects should be taken into account. The zero-temperature coherence length $\xi(0)$ is estimated to be about 4.94 nm by using $\xi(0) = [\varphi_0/(2\pi H_{c2}(0))]^{1/2}$, where $\varphi_0 = 2.07 \times 10^{-15}$ Wb is the flux quantum. In addition, through measuring the lower critical field H_{c1} and upper critical field H_{c2}, we can get the Ginzburg–Landau parameter $\kappa(1.9\text{ K})$ to be about 130 from

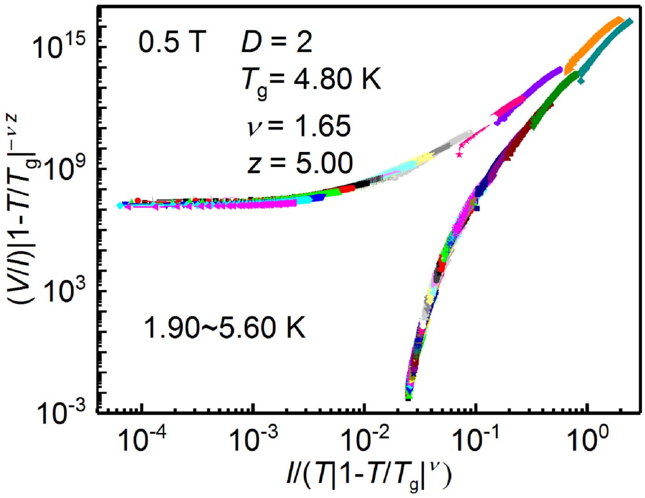

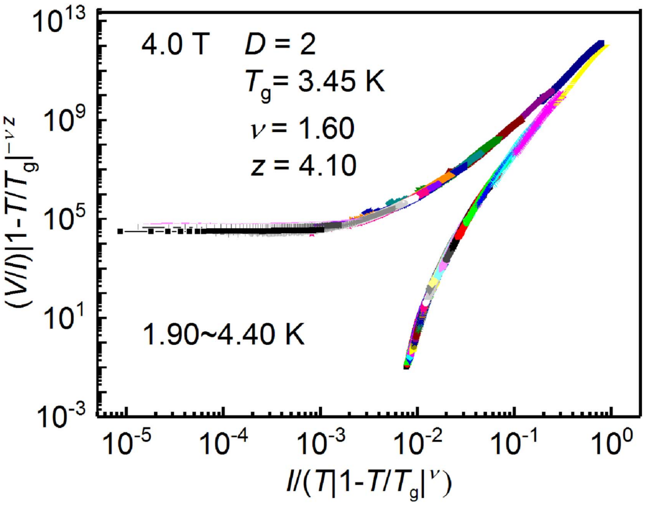

Figure 2. Quasi-2D VG scaling of *I–V* curves under magnetic fields of 0.5 T and 4.0 T.

Table 1. Quasi-2D VG scaling parameters at different fields.

H (T)	T_g (K)	z	ν
0.5	4.80	5.00	1.65
1	4.50	4.70	1.68
2	4.15	4.40	1.63
3	3.75	4.60	1.62
4	3.45	4.10	1.60
5	3.15	3.90	1.58
6	2.80	3.65	1.55
7	2.45	3.50	1.45

the equations of $H_{c2}(T) = \sqrt{2}\kappa(T)H_c(T)$ and $H_{c1}(T) = \frac{1}{\sqrt{2}\kappa(T)}H_c(T)(\ln\kappa(T) + 0.081)$ [32, 33], where H_c(T) is the thermodynamic critical field. Here, H_{c1}(1.9 K) is ~18 Oe from our earlier report [27], and H_{c2}(1.9 K) is ~12.30 T for the TiO thin films. Thus, the penetration depth λ(1.9 K) of about 673.4 nm can be estimated by the formula $\kappa(T) = \lambda(T)/\xi(T)$ with $\xi(1.9\text{ K}) \approx 5.18$ nm. Using formula $\lambda(T) = \lambda(0)[1 - (T/T_c)^4]^{-1/2}$ with $T_c = 6.63$ K (defined by the resistivity drop to 90% of the normal state resistance) [32], $\lambda(0) \approx 670.7$ nm could be obtained. Based on the VG scaling and the temperature-dependent resistance (*R–T*) curves, we constructed the vortex phase diagram of the TiO epitaxial thin films for magnetic fields perpendicular to the TiO film surface, as shown in figure 3(b). The vortex phase transition from a VG phase to a vortex liquid phase is separated by H_g (the vortex liquid–glass transition field [34]), which is close to H_{irr} [35]. The quasi-2D vortex phase diagram ranging from the VG and vortex liquid regions to the normal state of the TiO epitaxial thin films is comprehensive.

Furthermore, from the *I–V* characteristics, we obtained the temperature and magnetic field dependences of the critical current densities J_c (defined at $V = 10^{-6}$ V), as shown in figures 4(a)–(c), respectively. As we know, for a type-II superconductor, vortices would interact with pinning centers either via the spatial variations in T_c ('δT_c pinning') or by the scattering of charge carriers with reduced mean free path l near defects ('δl pinning') [22]. These two pinning types have different temperature dependences, and therefore result in different relationships between $J_c(t)$ and $t = T/T_c$ in the single vortex pinning regime (low-field regions) [30, 36]. For δT_c pinning, the critical current can be expressed as $J_c^{\delta T_c}(t) = J_c(0)(1 - t^2)^{7/6}(1 + t^2)^{5/6}$, while for δl pinning it is $J_c^{\delta l}(t) = J_c(0)(1 - t^2)^{5/2}(1 + t^2)^{-1/2}$ [24]. Taking the magnetic field for 5.0 T as an example, neither the δT_c (the green dashed line) nor the δl (the blue dashed line) pinning mechanism can fit J_c well, as shown in figure 4(a). Therefore, the J_c can be analyzed with the assumption of coexisting δT_c and δl pinning mechanisms within the following expression [37]:

$$J_c(t) = PJ_c^{\delta T_c}(t) + (1 - P)J_c^{\delta l}(t), \tag{4}$$

where P is a fitting parameter. Using equation (4), the experimental data can be well fitted with $P = 0.08$ in 5.0 T (the red dashed line), as shown in figures 4(a) and $P = 0.05 \sim 0.13$ in different magnetic fields, as shown in (b). This suggests that δl pinning, associated with variations in the charge carrier mean free path near lattice defects (e.g. grain boundaries, dislocation, or stacking faults) [22, 38], plays a main role in the critical current of the TiO thin films. These results can be understood because there are some grain boundaries and lattice defects in our sample [27]. Meanwhile, our earlier results also showed that the oxygen content in the film is not uniform.

To explain the mechanism of flux pinning in more detail, we studied the temperature and field dependences of the vortex pinning force $F_p = HJ_c$. Based on the Dew–Huges model [39], the magnetic field dependence of normalized vortex pinning forces F_p/F_p^{max} from different temperatures follows a scaling law:

$$F_p/F_p^{max} \propto h^p(1 - h)^q. \tag{5}$$

Here, h is a reduced field $h = H/H_{irr}$, and F_p^{max} corresponds to the maximum pinning force. The irreversibility field H_{irr} is the field where $J_c(T, H)$ extrapolates to 10 A cm^{-2} [40]. The indices p and q provide information about the pinning mechanism; $p = 0.64$, $q = 1.97$, and the peak position h_{max}^{fit}

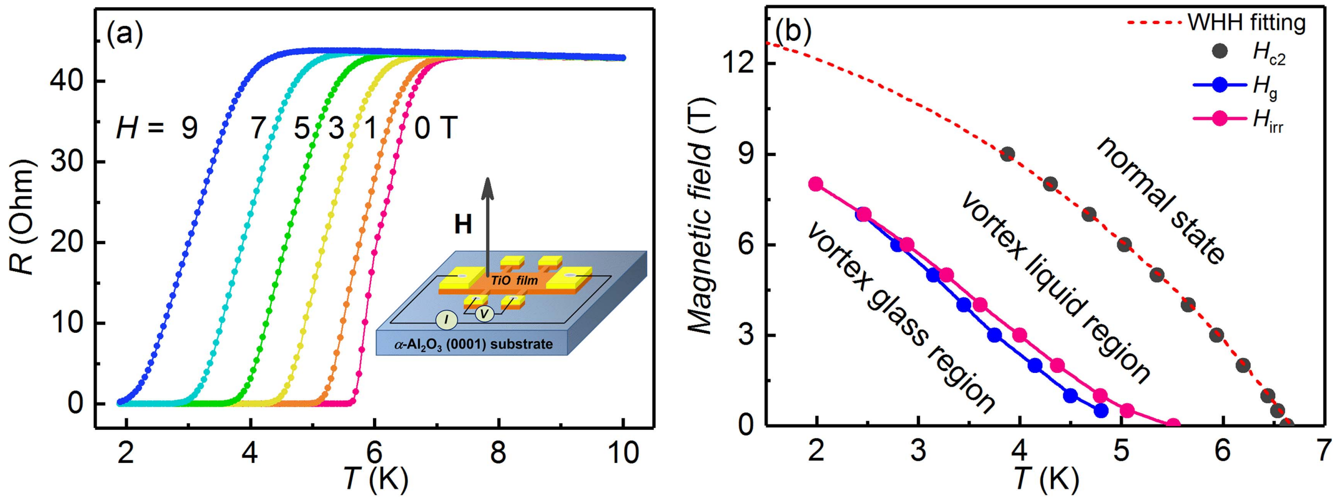

Figure 3. (a) Temperature dependences of the resistance R from 1.9 to 10 K in different magnetic fields; the inset is a schematic diagram of the experimental setup for the transport measurements. (b) Vortex phase diagram of TiO thin films for magnetic fields perpendicular to the film surface; the red dashed line is the fit to the WHH model.

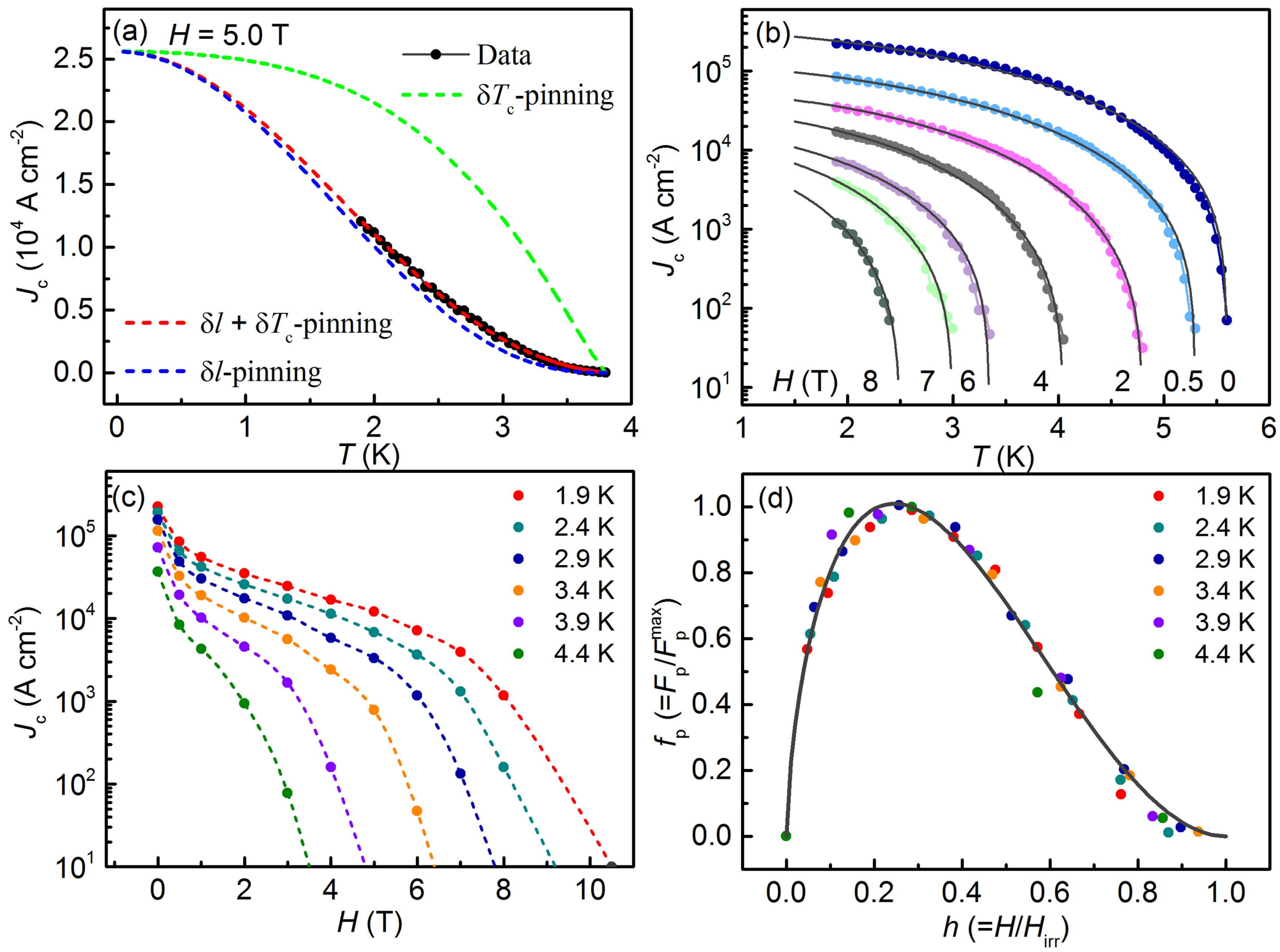

Figure 4. (a) Temperature dependence of the critical current densities J_c in a magnetic field of 5.0 T fitted by δT_c, δl, and $\delta T_c + \delta l$ pinning mechanisms, respectively. (b) Temperature dependences of the critical current densities J_c in different magnetic fields fitted by the $\delta T_c + \delta l$ pinning mechanism. (c) Critical current densities J_c versus H at different temperatures. (d) Reduced magnetic field dependences of the normalized flux pinning force at various temperatures. The solid line is the fitting curve using equation (5).

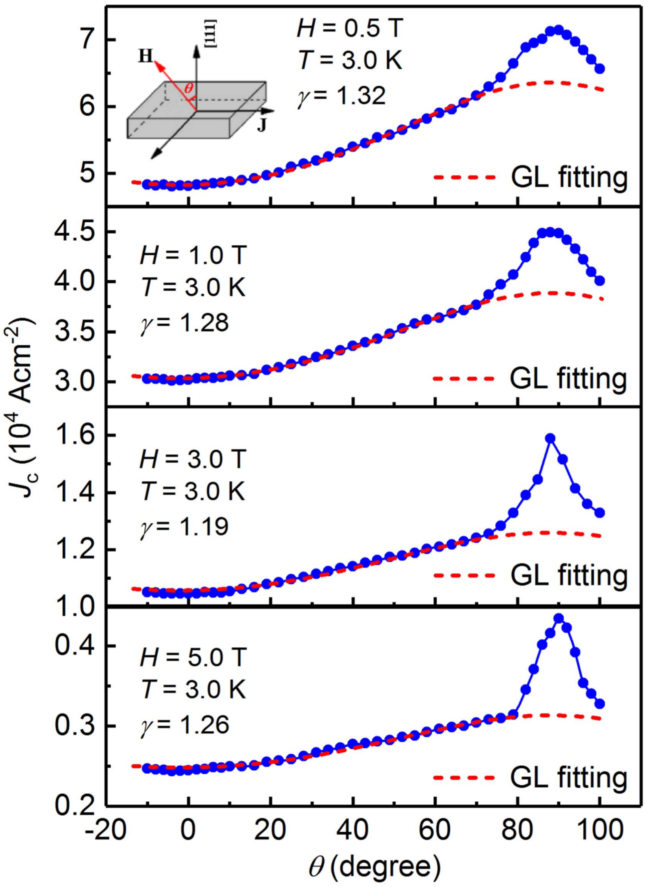

Figure 5. Angular dependences of J_c at 3.0 K in different magnetic fields; the red dashed lines represent the Ginzburg–Landau (GL) fitting results. The angle $\theta = 0°$ is defined as the applied magnetic field perpendicular to the surface of the TiO film ($H\perp(111)$), as shown in the inset.

$[=p/(p+q)] \approx 0.25$ were estimated using equation (5), as shown in figure 4(d). These values are close to the expected values for a normal surface-like pinning ($p = 1/2, q = 2$, and $h_{\max}^{\mathrm{fit}} = 0.2$) [39]. The solid line in figure 4(d) represents the curve shape expected for pinning by grain boundaries similar to those of MgB_2 [20, 41]. This consequence agrees with the results of analyzing pinning mechanisms through critical current densities.

Figure 5 shows the angular dependence of the critical current densities J_c. If the pinning is owing to uncorrelated defects randomly distributed over angular space, the angular dependence of J_c in different magnetic fields can be scaled by using the Ginzburg–Landau anisotropic scaling approach as follows [42]:

$$J_c(H, \theta) = J_c[H\varepsilon(\theta)], \tag{6}$$

where $\varepsilon(\theta) = [\cos^2(\theta) + \gamma_{Jc}^{-2}\sin^2(\theta)]^{1/2}$ and γ_{Jc} is the anisotropy parameter of J_c. The γ_{Jc} is about 1.3, which is larger than the anisotropy parameter $\gamma_{Hc2} \approx 1.04$ of the upper critical field $H_{c2}(0)$ (see supplementary information figure S1, available online at stacks.iop.org/SUST/31/015016/mmedia). The angle $\theta = 0°$ is defined as the applied magnetic field perpendicular to the TiO film surface ($H\perp(111)$), shown in the inset of figure 5. It is found that the angular dependences of J_c at 0.5 T, 1.0 T, 3.0 T, and 5.0 T follow equation (6) very well, except for a cusp-like behavior around the magnetic field parallel to the film surface. With increasing magnetic fields, the deviation becomes more obvious, and the cusp-like behavior looks sharper. The cusp properties may be caused by complicated pinning mechanisms related to the surface pinning [43, 44], vortex crossing reconnection [45], or image force effect [46].

4. Conclusions

The *I–V* characteristics and critical current density J_c in TiO epitaxial thin films were systematically studied. A quasi-2D VG phase transition was revealed by analyzing the scaling behaviors of the *I–V* characteristics. The temperature dependence of J_c at different fields indicated that δl pinning is the dominant pinning mechanism at the temperature range measured in the TiO thin films. In addition, a clear scaling behavior of the normalized field dependence of vortex pinning forces was observed.

Acknowledgments

This work was supported by the National Natural Science Foundation of China (51332007 and 51622209 and 21521001) and by the National Basic Research Program of China (2016YFA0300103, 2015CB921201 and 2012CB922003). Partial work was done at the USTC Center for Micro- and Nanoscale Research and Fabrication at the University of Science and Technology of China, Hefei, China.

ORCID iDs

Xiaoguang Li https://orcid.org/0000-0003-4016-4483

References

[1] Marcenat C, Demuer A, Beauvois K, Michon B, Grockowiak A, Liang R, Hardy W, Bonn D A and Klein T 2015 Calorimetric determination of the magnetic phase diagram of underdoped ortho II $YBa_2Cu_3O_{6.54}$ single crystals *Nat. Commun.* **6** 7927

[2] Teng M L, Zhang M J, Hao F X, Yin Y W and Li X G 2015 Nanoscale-phase-separation–enhanced critical current and vortex transition temperature in $K_{0.62}Fe_{1.71}Se_2$ crystals *Europhys. Lett.* **111** 37001

[3] Shahbazi M, Wang X L, Ghorbani S R, Ionescu M, Shcherbakova O V, Wells F S, Pan A V, Dou S X and Choi K Y 2013 Vortex-glass phase transition and enhanced flux pinning in C^{4+}-irradiated $BaFe_{1.9}Ni_{0.1}As_2$ superconducting single crystals *Supercond. Sci. Tech.* **26** 095014

[4] Heron D O, Ray S J, Lister S J, Aegerter C M, Keller H, Kes P H, Menon G I and Lee S L 2013 Muon-spin rotation measurements of an unusual vortex-glass phase in the layered superconductor $Bi_{2.15}Sr_{1.85}CaCu_2O_{8+\mathrm{delta}}$ *Phys. Rev. Lett.* **110** 107004

[5] Hao F X, Zhang M J, Teng M L, Yin Y W, Jiao W H, Cao G H and Li X G 2015 Angle-resolved vortex glass transition and pinning properties in $BaFe_{1.8}Co_{0.2}As_2$ single crystals *J. Appl. Phys.* **117** 173901

[6] Shahbazi M, Wang X L, Choi K Y and Dou S X 2013 Flux pinning mechanism in $BaFe_{1.9}Ni_{0.1}As_2$ single crystals: evidence for fluctuation in mean free path induced pinning *Appl. Phys. Lett.* **103** 032605

[7] Zhang Y Q, Ding J F, Xiang X Q, Li X G and Chen Q H 2009 Effect of stripe order on the vortex phase transition in $La_{1.44}Nd_{0.4}Sr_{0.16}CuO_4$ films *Supercond. Sci. Tech.* **22** 085010

[8] Dietel J and Kleinert H 2007 Phase diagram of vortices in high-T_c superconductors from lattice defect model with pinning *Phys. Rev.* B **75** 144513

[9] Chang H H, Luo J Y, Wu C T, Hsu F C, Huang T W, Wu P M, Wu M K and Wang M J 2011 The vortex state of $FeSe_{1-x}Te_x$ superconducting thin films *Supercond. Sci. Tech.* **24** 105011

[10] Kim K H, Kang W, Kim M-S, Jung C, Kim H-J, Choi E-M, Park M-S and Lee S-I 2002 Negligible effect of grain boundaries on the supercurrent density in polycrystalline MgB_2 *Physica* C **370** 13–6

[11] Gupta S K *et al* 2002 $I-V$ characteristic measurements to study the nature of the vortex state and dissipation in MgB_2 thin films *Phys. Rev.* B **66** 104525

[12] Yang H, Jia Y, Shan L, Zhang Y, Wen H-H, Zhuang C, Liu Z, Li Q, Cui Y and Xi X 2007 $I-V$ characteristics of the vortex state in MgB_2 thin films *Phys. Rev.* B **76** 134513

[13] Sefrioui Z, Arias D, Varela M, Villegas J E, de la Torre M A L, Leon C, Loos G D and Santamaria J 1999 Crossover from a three-dimensional to purely two-dimensional vortex-glass transition in deoxygenated $YBa_2Cu_3O_{7-\delta}$ thin films *Phys. Rev.* B **60** 15423–9

[14] Yamasaki H, Endo K, Kosaka S, Umeda M, Yoshida S and Kajimura K 1994 Quasi-two-dimensional vortex-glass transition observed in epitaxial $Bi_2Sr_2Ca_2Cu_3O_x$ thin films *Phys. Rev.* B **50** 12959–65

[15] Wen H H, Ziemann P, Radovan H and Yan S 1998 Field-induced crossover of criticalities of vortex dynamics in $Tl_2Ba_2CaCu_2O_8$ thin films *Europhys. Lett.* **42** 319–24

[16] Zhang Y Z, Deltour R, de Marneffe J F, Wen H H, Qin Y L, Dong C, Li L and Zhao Z X 2000 Vortex characteristics in a superconducting $Bi_2Sr_{2-x}La_xCuO_{6+\delta}$ thin film *Phys. Rev.* B **62** 11373–6

[17] Mawatari Y, Yamasaki H, Kosaka S and Umeda M 1995 Critical current properties and vortex-glass-liquid transition in Ag-sheathed Bi-2223 tapes *Cryogenics* **35** 161–7

[18] Li Q, Wiesmann H, Suenaga M, Motowidlo L and Haldar P 1995 Vortex phase diagram and J_c limiting factor in high T_c $Bi_2Sr_2Ca_2Cu_3O_{10}/Ag$ superconducting tapes *Appl. Phys. Lett.* **66** 637–9

[19] Villegas J E and Vicent J L 2005 Vortex-glass transitions in low-T_c superconducting Nb thin films and Nb/Cu superlattices *Phys. Rev.* B **71** 144522

[20] Larbalestier D C *et al* 2001 Strongly linked current flow in polycrystalline forms of the superconductor MgB_2 *Nature* **410** 186–9

[21] Laviano F, Gerbaldo R, Ghigo G, Gozzelino L, Mikitik G P, Taen T and Tamegai T 2014 Evidence of anisotropic vortex pinning by intrinsic and irradiation-induced defects in $Ba(Fe,Co)_2As_2$ studied by quantitative magneto-optical imaging *Supercond. Sci. Tech.* **27** 044014

[22] Blatter G, Feigel'man M V, Geshkenbein V B, Larkin A I and Vinokur V M 1994 Vortices in high-temperature superconductors *Rev. Mod. Phys.* **66** 1125–388

[23] Zhang M J, Teng M L, Hao F X, Yin Y W, Li X G and Zeng Z 2014 Influence of spin injection on the critical current density in $La_{0.7}Sr_{0.3}MnO_3/La_{1.85}Sr_{0.15}CuO_4$ heterostructure *AIP Adv.* **4** 127138

[24] Griessen R, Wen H-H, van Dalen A J, Dam B, Rector J, Schnack H G, Libbrecht S, Osquiguil E and Bruynseraede Y 1994 Evidence for mean free path fluctuation induced pinning in $YBa_2Cu_3O_7$ and $YBa_2Cu_4O_8$ films *Phys. Rev. Lett.* **72** 1910–3

[25] Wang D, Huang C, He J, Che X, Zhang H and Huang F 2017 Enhanced superconductivity in Rock-Salt TiO *ACS Omega* **2** 1036–9

[26] Liu X, Zhang C, Hao F X, Wang T Y, Fan Y J, Yin Y W and Li X G 2017 Hydrostatic pressure effect on the transport properties in TiO superconducting thin films *Phys. Rev.* B **96** 104505

[27] Zhang C, Hao F X, Gao G Y, Liu X, Ma C, Lin Y, Yin Y W and Li X G 2017 Enhanced superconductivity in TiO epitaxial thin films *NPJ Quantum Mater.* **2** 2

[28] Zhang M J, Teng M L, Hao F X, Yin Y W, Zeng Z and Li X G 2015 Effect of injected spins with different polarized orientations on the vortex phase transition in $La_{0.7}Sr_{0.3}MnO_3/La_{1.85}Sr_{0.15}CuO_4$ heterostructure *J. Appl. Phys.* **117** 17E118

[29] Fisher D S, Fisher M P A and Huse D A 1991 Thermal fluctuations, quenched disorder, phase transitions, and transport in type-II superconductors *Phys. Rev.* B **43** 130–59

[30] Prozorov R *et al* 2008 Vortex phase diagram of $Ba(Fe_{0.93}Co_{0.07})_2As_2$ single crystals *Phys. Rev.* B **78** 224506

[31] Werthamer N R, Helfand E and Hohenberg P C 1966 Temperature and purity dependence of the superconducting critical field,H_{c2}. III. Electron spin and spin–orbit effects *Phys. Rev.* **147** 295–302

[32] Charles P, Poole J, Farach H A, Creswick R J and Prozorov R 2007 *Superconductivity* (London: Academic)

[33] Abrikosov A A 1957 On the magnetic properties of superconductors of the second group *Sov. Phys. JETP* **5** 1174–83

[34] Koch R H, Foglietti V V, Gallagher W J, Koren G, Gupta A and Fisher M P 1989 Experimental evidence for vortex-glass superconductivity in Y-Ba-Cu-O *Phys. Rev. Lett.* **63** 1511–4

[35] Nishizaki T and Kobayashi N 2000 Vortex-matter phase diagram in $YBa_2Cu_3O_y$ *Supercond. Sci. Tech.* **13** 1–11

[36] Thompson J R, Sun Y R, Civale L, Malozemoff A P, McElfresh M W, Marwick A D and Holtzberg F 1993 Effect of flux creep on the temperature dependence of the current density in Y-Ba-Cu-O crystals *Phys. Rev.* B **47** 14440–7

[37] Lei H and Petrovic C 2011 Giant increase in critical current density of $K_xFe_{2-y}Se_2$ single crystals *Phys. Rev.* B **84** 212502

[38] Wördenweber R 1999 Mechanism of vortex motion in high-temperature superconductors *Rep. Prog. Phys.* **62** 187–236

[39] Dew-Hughes D 2006 Flux pinning mechanisms in type II superconductors *Philos. Mag.* **30** 293–305

[40] Su T S, Yin Y W, Teng M L, Zhang M J and Li X G 2014 Angular dependence of vortex dynamics in $BaFe_{1.9}Ni_{0.1}As_2$ single crystal *Mater. Res. Express* **1** 016003

[41] Dew-Hughes D 1987 The role of grain boundaries in determining J_c in high-field high-current superconductors *Philos. Mag.* **55** 459–79

[42] Iida K, Hänisch J, Thersleff T, Kurth F, Kidszun M, Haindl S, Hühne R, Schultz L and Holzapfel B 2010 Scaling behavior of the critical current in clean epitaxial $Ba(Fe_{1-x}Co_x)_2As_2$ thin films *Phys. Rev.* B **81** 100507 (R)

[43] Khokhlov V A, Kosse A I, Kuzovlev Y E, Levcihenko G G, Medvedev Y V, Prokhorov A Y, Mikheenko P, Chakalov R and Muirhead C M 2004 Surface pinning as

origin of high critical current in superconducting films *Supercond. Sci. Tech.* **17** S520–3
[44] Sun Y R, Thompson J R, Kerchner H R, Christen D K, Paranthaman M and Brynestad J 1994 Strong surface-pinning effects in polycrystalline $HgBa_2CuO_{4+\delta}$ superconductors *Phys. Rev.* B **50** 3330–6
[45] Vlasko-Vlasov V K, Colauto F, Buzdin A A, Carmo D, Andrade A M H, Oliveira A A M, Ortiz W A, Rosenmann D and Kwok W K 2016 Crossing fields in thin films of isotropic superconductors *Phys. Rev.* B **94** 184502
[46] Deblois R W and Desorbo W 1964 Surface barrier in type-II superconductors *Phys. Rev. Lett.* **12** 14–6